Author(s): Sissaoui, Jihad; Efimov, Alexander; Kumpulainen, Tatu; Vauthey, Eric

Title: Photoinduced Electron Transfer in a Porphyrin-Fullerene Dyad at a Liquid Interface

Year: 2022

Version: Accepted version (Final draft)

Please cite the original version:

Sissaoui, J., Efimov, A., Kumpulainen, T., & Vauthey, E. (2022). Photoinduced Electron Transfer in a Porphyrin-Fullerene Dyad at a Liquid Interface. Journal of Physical Chemistry B, 126(25), 4723-4730. https://doi.org/10.1021/acs.jpcb.2c02405

Photoinduced Electron Transfer in a Porphyrin-Fullerene Dyad at a Liquid Interface

Jihad Sissaoui,[†] Alexander Efimov,[‡] Tatu Kumpulainen,[*,¶] and Eric Vauthey[*,†]

[†]*Department of Physical Chemistry, University of Geneva, 30 Quai Ernest-Ansermet, Geneva, Switzerland*

[‡]*Faculty of Engineering and Natural Sciences, Tampere University, Korkeakoulunkatu 8, Tampere, Finland*

[¶]*Department of Chemistry/Nanoscience Center, University of Jyväskylä, Survontie 9 C, Jyväskylä, Finland*

E-mail: tatu.s.kumpulainen@jyu.fi; eric.vauthey@unige.ch

Abstract

The excited-state properties of an amphiphilic porphyrin-fullerene dyad and of its porphyrin analogue adsorbed at the dodecane/water interface are investigated using surface second-harmonic generation. Although the porphyrin is formally centro-symmetric, the second-harmonic spectra of both compounds are dominated by the intense Soret band of the porphyrin. Polarisation-selective measurements and molecular dynamics simulations suggest an angle of about 45° between the donor-acceptor axis and the interfacial plane, with the porphyrin interacting mostly with the non-polar phase. Time-resolved measurements reveal a marked concentration dependence of the dynamics of both compounds upon Q-band excitation, indicating the occurrence of intermolecular quenching processes. The significant differences in dynamics and spectra between the dyad and the porphyrin analogue are explained by a self-quenching of the excited dyad via an intermolecular electron transfer.

Introduction

Interfaces between two immiscible liquids are involved in many areas of science and technology.[1–7] Because the molecules experience an asymmetry of forces at the interface, their orientation is not isotropic, giving rise to properties that can significantly differ from those of the two constituting liquids. This, in turn, can have a strong impact on the chemical reactivity. These specific properties of liquid interfaces are exploited in 'on-water' chemistry, where reactions between organic reactants are accelerated in the presence water.[8–13] However, the current understanding of the chemical dynamics at liquid interfaces is still limited. This is mostly due to their typical thickness of 1-2 nm, and, consequently, to the extremely small number of molecules in this region relative to those in the bulk phases. Therefore, the spectroscopic response from the interface is usually buried in the response arising from the bulk, unless a surface-selective technique is used.

Herein, we report on our investigation of the excited-state properties of an electron donor-acceptor dyad at the dodecane/water interface using surface second-harmonic generation (SSHG). Despite the relevance of interfacial charge-transfer processes, this technique has still been rarely applied for studying the dynamics of photoinduced electron transfer at liquid interfaces.[14,15] SSHG is selective to the interface between two isotropic media as its probes the second-order non-linear optical susceptibility, $\overleftrightarrow{\chi}^{(2)}$, which, under the dipolar ap-

proximation, is zero in centro-symmetric materials.[16–21] The magnitude of the tensor elements of $\overleftrightarrow{\chi}^{(2)}$ is strongly frequency dependent and its spectrum consists of bands arising from one- and two-photon resonances. We exploit the electronic resonance enhancement so that the second-harmonic (SH) signal originates only from the dyad and not from dodecane or water molecules.

The dyad **1** consists of a free-base tetraphenyl porphyrin (H_2TPP) doubly linked to a C_{60} fullerene (Chart 1). Substitution on the porphyrin and fullerene sub-units confers an amphiphilic character, as shown by a previous study, where Langmuir-Blodgett monolayers of this dyad were prepared.[22] According to previous time-resolved studies,[23–25] local excitation of the porphyrin sub-unit is followed by the ultrafast population of a delocalised excited state interpreted as an exciplex.[26] In polar solvents, the latter evolves in a few picoseconds into a charge-separated state with a sub-nanosecond lifetime. In non-polar media, the exciplex decays back to the ground state on a few nanoseconds timescale.

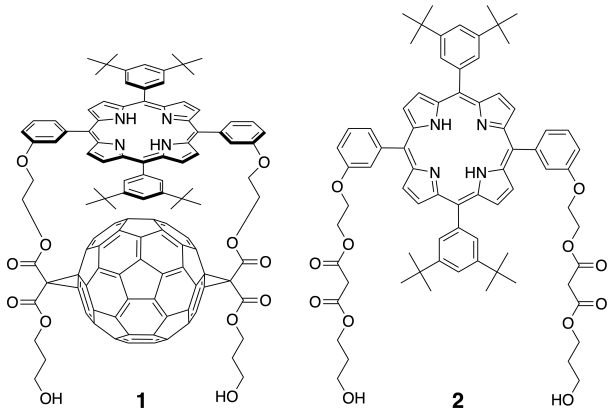

Chart 1: Structure of the dyad **1** and of the porphyrin-only analogue **2**.

We compare the excited-state dynamics of the dyad with those of the donor phorphyrin analogue (**2**, Chart 1) using time-resolved SSHG. Information on the orientation of these two molecules at the interface is obtained by using both polarised SSHG and molecular dynamics (MD) simulations. The results suggest that the excited-state dynamics of both compounds at the interface is dominated by self-quenching processes, which, in the case of the dyad, involve intermolecular charge separation. In this respect, these interfacial dynamics differ significantly from those measured in solution.

Methods

Samples

The synthesis of the dyad **1** and of the reference compound **2** was reported in ref. 27. Dodecane (99+%) was purchased from Alfa Aesar. Water was purified using a Milli-Q Reference system before use.

The samples were prepared by adding a specific volume (between 0.5 to 7 μL) of a 0.1 mM solution of the dye in $CHCl_3$ on the lower aqueous phase located in a 4x4x4 cm^3 cubic quartz cell. Dodecane was slowly added after approximately 10 min., allowing the $CHCl_3$ to evaporate. All measurements were performed at room temperature.

Surface second harmonic generation

Experimental setup. The SSHG setup, was based on a 1 kHz amplified Ti:Sapphire system (Solstice, Spectra-Physics) and was described in detail before.[28,29] Briefly, the SSHG probe pulses (100 fs, 0.7 μJ and 130 μm x 340 μm spot-size at the interface) were generated with a collinear optical parametric amplifier (Topas C, Light Conversion), and were focussed onto the interface with an angle of incidence just above the critical angle for total internal reflection, which amounts to about 70° for the dodecane/water interface between 350 and 1200 nm. Their polarisation was controlled with a half-wave plate. The conventional notation for the polarisation is used: p for parallel polarization with respect to the plane of incidence, s for perpendicular polarisation and 45°. The reflected pulses were guided through a combination of irises, filter and spectrograph to eliminate the reflected probe light before reaching a CCD camera (Newton 920, Andor). No SH signal could be detected at the dodecane/water

without the dye.

Stationary second-harmonic spectra. Stationary SH spectra were recorded by scanning the wavelength of the probe pulses with 5 nm steps. They were measured at $\gamma = 45°/s$ polarisation geometry. The spectra were corrected using the SH spectrum from a Al mirror immersed in dodecane.[30] The resulting spectral intensity is referred to as I_{SH}. The SH spectra are usually displayed using $\sqrt{I_{SH}}$, as this quantity is proportional to the concentration of harmonophores.

Polarization-resolved SSHG. For polarization selective measurements, the polarisation angle of the incident beam at 860 or 840 nm, γ, was controlled with a half-wave plate mounted on a motorised rotatory stage and a given polarisation component of the steady-state SH signal was selected using a wire-grid polariser.[30] The resulting signal intensity is referred to as I_{SH}.

Time-resolved SSHG. For TR-SSHG measurements, a pump pulse channel that can be delayed with respect to the probe pulse was added to the SSHG setup. The pump pulses were at 520 nm (80 fs, 0.8 μJ and 180 μm x 500 μm spotsize at the interface) and were generated with a noncollinear optical parametric amplifier (Topas White, Light Conversion). This wavelength corresponds to the Q_y transition of the porphyrin sub-unit. These pulses were circularly polarized to avoid photoselection and were focused on the interface from the top using a combination of spherical and cylindrical lenses and overlapped with the probe pulses. As a consequence, the SH signal is resonant with the Soret band transition of the porphyrin sub-unit.

The TR-SSHG profiles were recorded using the $45°/s$ polarization, where the signal intensity is the highest. No significant dependence of the dynamics on the polarization was observed. In order to correct for the fluctuations of the probe beam intensity, a chopper was used to reduce the pump pulse repetition rate by a factor of 2 relative to the probe pulse. The reflected SH signal was directed onto the spectrograph entrance slit using a mirror mounted on a galvanometer oscillating at the same frequency (500 Hz). The SH signals coming from the pumped and the un-pumped sample hit different spots on the CCD camera and were measured separately. The TR-SSHG profiles were processed by taking the square root of the pumped SH signal intensity divided by the square root of the non-pumped signal intensity, and were then normalised, so that it changes from 1 to 0 upon photoexcitation. As the SSHG is purely resonant, the resulting signal, $S(t)$, directly reflects the photoinduced changes in population.

Molecular dynamics simulations

Molecular dynamics (MD) simulations were carried out using GROMACS 2021.2.[31] The topology files for **1** and **2**, based on the AMBER99SB-ILDN force field,[32,33] were generated using the Antechamber Python parser interface (ACPYPE) tool,[34] with as input the optimised structures obtained from DFT quantum-chemical calculations (B3LYP/6-31G+d)[35] as implemented in the Gaussian 16 package.[36] For the dyad **1**, the force field parameters of the fullerene were taken from ref. 37. The atomic charges were determined from CHELPG fits of the electrostatic potential obtained from the DFT calculations.[38] The TIP3P model was used for water,[39] whereas, for dodecane, the atom types obtained from ACPYPE were changed to distinguish two different sets of carbon and hydrogen types for the CH_3 and CH_2 groups with the Lennard-Jones parameters taken from ref. 40. Without this modification, the simulated dodecane freezes at room temperature.[41] A periodic rectangular box (6x6x11 nm^3) with two dodecane/water interfaces was used for the simulations. It contained 512 dodecane molecules, and either 5850 water molecules and two dyads or 5906 water molecules and two porphyrin-only dyes **2**. Simulations were performed at constant pressure and temperature (295 K) with 2 fs steps for 40 to 150 ns. Further details on the simulation parameters can be found in the Supporting Information.

Results and discussion

Origin of the SH signal. The stationary SH spectra recorded with **1** and **2** at the dodecane/water interface are compared with their electronic absorption spectra in $CHCl_3$ in Figure 1. The SH spectra are dominated by a band peaking at 428 nm, that can be assigned to an electronic resonance associated with the Soret band of the H_2TPP sub-unit. The larger width of this SH band compared to the corresponding absorption band is mostly due to the ∼10 nm spectral width of the SH probe pulse.

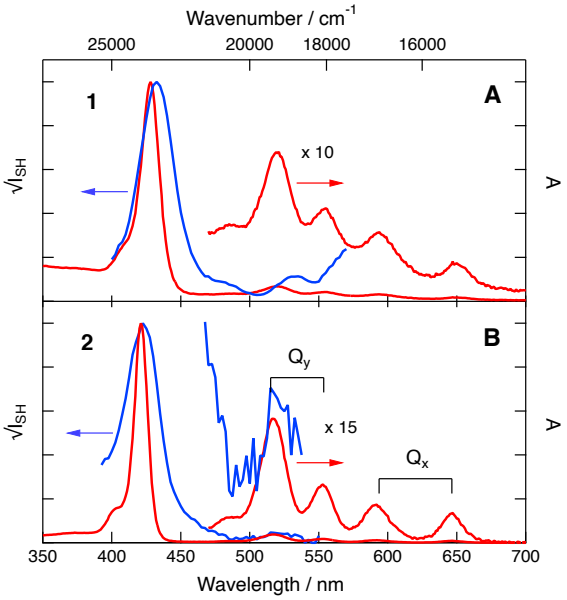

Figure 1: Stationary electronic absorption and SH spectra recorded with **1** (A) and **2** (B) in $CHCl_3$ and at the dodecane/water interface.

Both the SH and absorption bands of the dyad **1** are red shifted by about 400 cm^{-1} relative to those of the reference porphyrin **2**. Furthermore, the absorption band of **1** markedly broader than that of **2**, i.e. 930 vs. 620 cm^{-1}. The Soret band is due to two quasi-degenerate porphyrin transitions,[42] and the larger width with **1** was attributed to interactions with the fullerene sub-unit, which lead to an increased energy splitting of these two transitions.[23] In principle, centro-symmetric molecules like porphyrins do not have any non-zero element of the hyperpolarisability tensor, $\overleftrightarrow{\beta}$, and should thus not give any SH signal.[43] However, the SH response from porphyrins is well-documented,[44–48] and has been explained by structural distortions in the asymmetric interfacial environment, resulting in non-zero tensor elements of $\overleftrightarrow{\beta}$. However, the dyad is not centro-symmetric and, according to quantum-chemical calculations described in the Supporting Information (Section S2), it has a non-zero $\overleftrightarrow{\beta}$. The same is also true for **2**, because of the long-chain substituents that are oriented toward the aqueous phase. These calculations suggest that $\overleftrightarrow{\beta}$ becomes particularly large when the SHG signal is resonant with the Soret band transitions, in agreement with the observations. The SH spectra of both **1** and **2** show also weaker features above 500 nm that can be associated with the Q bands. The relative intensity of these features is significantly larger for **1** than for **2**. This could be attributed to perturbations of the electronic structure of the porphyrin due to the presence of the fullerene sub-unit and/or to a contribution to the SH signal from the fullerene, which has electronic resonances in this spectral region.[49]

Independently on the origin of the difference between the electronic absorption and SH spectra, these results confirm that both **1** and **2** are located at the interface and are responsible for the measured SH signal. This is further confirmed by the absence of a signal without dye at the dodecane/water interface.

Orientation at the interface. Polarisation-resolved SSHG measurements were performed to get information on the orientation of **1** and **2** at the interface. Figure 2 shows polarisation profiles obtained upon measuring the intensity of three polarisation components of the SH signal, namely parallel (p), perpendicular (s), and at 45° relative to the plane of incidence, as a function of the polarisation angle of the probe field, γ. The p and 45° profiles recorded with **1** and **2** are markedly distinct. They point to differences in the symmetry of the second-order nonlinear susceptibility tensor:[16,17]

$$\overleftrightarrow{\chi}^{(2)} \propto N\langle\overleftrightarrow{\beta}\rangle, \qquad (1)$$

where N is the surface density of the dyes and

the angle brackets denote orientational averaging. Analysis of these profiles allows for the determination of the relative magnitude of the three independent non-zero tensor elements of $\overleftrightarrow{\chi}^{(2)}$ (see Supporting Information Section S1 for details).[17,50–53] The latter can, in turn, be used to estimate the orientation parameter D:

$$D = \frac{\langle \cos^3 \theta \rangle}{\langle \cos \theta \rangle}, \qquad (2)$$

where θ is the tilt angle between the transition dipole moment associated with the resonance probed by SSHG and the normal to the interface. In order to do this, the dominant elements of the hyperpolarisability tensor have to be known. Given that the SH signal is due to the porphyrin sub-unit, chemical intuition suggests that the dominant tensor elements should be associated with the porphyrin plane, where the transition dipoles are located. This is confirmed by quantum-chemical calculations of $\overleftrightarrow{\beta}(-2w, w, w)$ with $2w$ corresponding to the Soret band transition frequency, which suggest that the dominant tensor elements are β_{zzz} and β_{zxx}, with the molecular-frame axes x and z located in the plane (see Supporting Information, Section S2). With this definition, θ is the angle between the porphyrin plane and the normal to the interface.

Analysis of the polarisation curves, assuming a delta distribution of the tilt angle, yield θ values of 45° and 56° for **1** and **2**, respectively. This indicates that the orientation of the dyad **1** is such that its porphyrin sub-unit lies less flat at the interface than the reference **2**.

Figure 3A depicts snapshots of **1** and **2** at the dodecane/water interface taken from 40 to 150 ns MD simulations. Both molecules were initially inserted in the aqueous phase, and moved to the interface within 1 ns. After this period, they remained adsorbed at the interface during the whole simulation time. These snapshots reveal that the porphyrin and the fullerene sub-units of the dyad, both of which are hydrophobic, are mostly located in the dodecane phase and that interaction with the aqueous phase occurs mainly via the two hydrophilic chains. This is confirmed by density

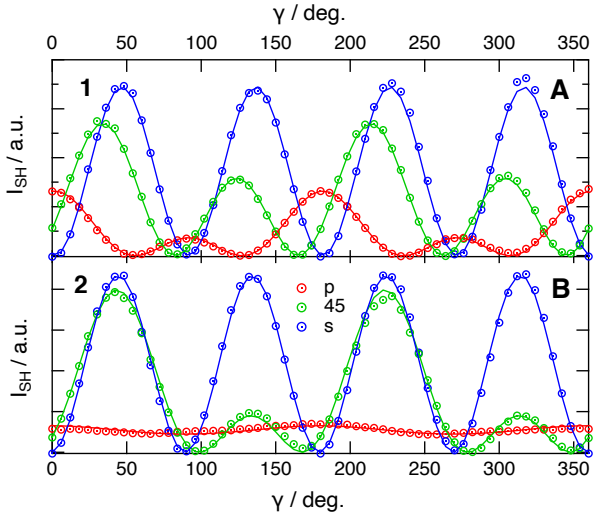

Figure 2: Polarisation-resolved SH profiles recorded at γ/x (x=p, 45 or s) geometries with **1** (A, 430 nm) and **2** (B, 420 nm) at the dodecane/water interface. The solid lines are best fits of eq.S2-S4.

profiles (Figure S3) that indicate that the density associated with **1** is not distributed symmetrically relative to the interface plane, but is centered on the dodecane side.

The most probable orientation of the dyad with the porphyrin plane at about 40° from the interface normal minimises the contact of the two hydrophobic sub-units with water while keeping the end of both arms in an aqueous environment. Figure 3B shows histograms of the tilt angle θ of **1** extracted from the last 100 ns of two 150 ns trajectories. The small differences between these two distributions point to slow fluctuations of the orientation, which would require very long simulation times to be properly sampled. Given the similarity of these two distributions, we assume that their sum, also presented in this figure, accounts reasonably well for the orientation of the dyad. It can be reproduced using a Gaussian function centred at 43° with a 16° root means square (rms) width.

In the case of the analogue **2**, 40 ns trajectories were sufficient to obtain identical histograms of the tilt angle, with a maximum at 76° (Figure 3C). They can be reproduced using a skewed Gaussian function with a rms width of 13°. As illustrated in Figure 3A, the porphyrin plane of **2** lies almost flat at the interface, with

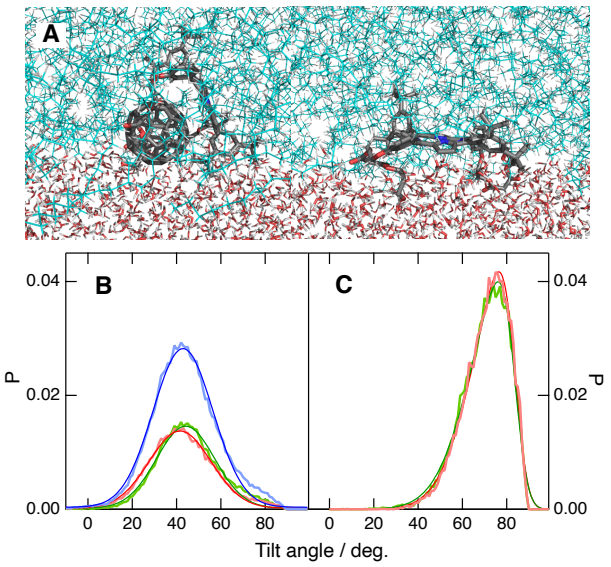

Figure 3: Snapshots from MD simulations of the dyad **1** and the porphyrin reference **2** at the dodecane/water interface (A); distributions of tilt angle θ obtained from two 100 ns (for **1**, B) and 40 ns (for **2**,C) trajectories. The blue curve in B is the sum of the two distributions.

the hydrophilic chains penetrating in the aqueous sub-phase. Although slightly centred on the dodecane side, the density profile of dye **2** extends less in this phase than that of the dyad (Figure S3).

The difference of tilt angle deduced from the polarisation curves and the MD simulations of **2** can to a large extent be explained by the assumption of a delta distribution of θ, which is not supported by the MD simulations. As discussed by Simpson and Rowlen,[54] a Gaussian distribution of θ centred at 76° with a width of 16° should give an apparent tilt angle of about 60 ° when assuming delta distribution (Figure S1). This is in better agreement with the 56° value determined from the polarisation profiles. The effect of a distribution decreases as the centre of this distribution approaches 39.2°.[54] For this reason, a 13° wide distribution of θ around 43°, as found for the dyad, should give a similar apparent angle (Figure S1).

Excited-state dynamics. Figure 4A shows time-resolved (TR) SH profiles, $S(t)$, recorded at 430 nm upon 520 nm excitation of the dyad **1** at different concentrations at the water/dodecane interface. Those measured with **2** at 420 nm are shown for comparison (Figure 4 B). As mentioned above, $S(t)$ reflects the photoinduced change in population. This approximation is valid here because the signal is purely resonant.

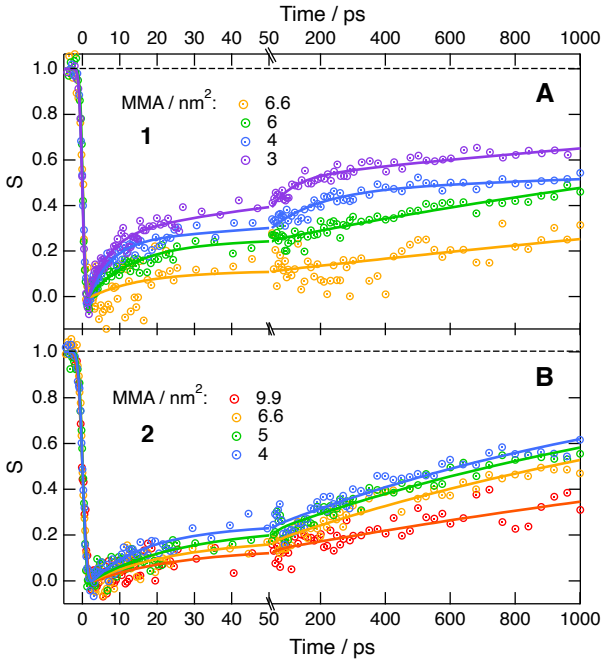

Figure 4: Time-resolved SSHG signal, $S(t)$, profiles recorded at 430 nm (**1**) or 420 nm (**2**) after 520 nm excitation of the dyad **1** (A) or the porphyrin analogue **2** (B) at different concentrations, expressed in mean molecular area (MMA), at the dodecane/water interface. The solid lines are best multiexponential fits.

As an alternative to concentration, we use the mean molecular area, MMA, i.e. the interfacial area available per dye molecule, calculated assuming that all dyes are adsorbed. Full coverage of the interface can be estimated to correspond to a MMA of about 3 nm^2.[22]

For both molecules, photoexcitation in the Q band region leads to a prompt decrease of the SH intensity. The ensuing recovery dynamics of $S(t)$ are accelerated with increasing dye concentration for both **1** and **2**. At the lowest concentration (highest MMA), the signal recovers by only about 20-30% after 1 ns. As the concentration is increased (MMA decreased), the amount of recovery becomes larger due to the presence

of fast components. For the dyad, these faster dynamics of $S(t)$ can be reproduced using exponential functions with ∼5 and ∼100 ps time constants (Table S3). For the reference **2**, a single exponential function with a ∼20 ps time constant is sufficient to reproduce the initial dynamics. At a given concentration, the signal recovery 1 ns after excitation is systematically smaller for the dyad than for the reference.

As the stationary SH signal in the 420-430 nm region is resonant with the Soret band transition, its intensity is proportional to the square of the ground-state population, namely, $I_{SH} \propto |N_{S0}\langle\beta_{S0}\rangle|^2$, where β_{S0} is the hyperpolarisability tensor of the dye in the electronic ground state. Photoexcitation at 520 nm in the Q_y band of the porphyrin leads to the population of the S_1 state, which can then either decay back to the ground state or populate another state X. The signal intensity is:

$$I_{SH}(t) \propto |N_{S0}(t)\langle\beta_{S0}\rangle + N_{S1}(t)\langle\beta_{S1}\rangle + N_X(t)\langle\beta_X\rangle|^2,$$

where N_i and β_i are the population and hyperpolarisability tensor of state i, respectively. Given that directly after excitation, only the S_0 and the S_1 states are populated, the decrease of the SH intensity, hence of $S(t)$, indicates that $\beta_{S0} > \beta_{S1}$. This agrees with electronic transient absorption measurements, which demonstrate that H_2TPP has relatively weak $S_n \leftarrow S_1$ absorption between 440 and 700 nm.[55,56] The recovery of the signal could have two origins: 1) the repopulation of the ground state or 2) the population of a state X with $\beta_X > \beta_{S1}$ at the probe wavelength.

The excited-state dynamics of the reference compound in bulk solution can be expected to be similar to those of H_2TPP, namely, the S_1 state decays via internal conversion and fluorescence to the ground state and via inter-system crossing (ISC) to the T_1 state. In toluene, the fluorescence lifetime of H_2TPP amounts to 12.8 ns and its triplet yield to 0.8.[57] On the other hand, a fluorescence lifetime of 7.9 ns was measured with **2** in $CHCl_3$ (Figure S7). Based on this, the $S(t)$ signal measured with **2** should recover by less than 20% within 1 ns. The faster dynamics measured experimentally, and especially its strong concentration dependence are most probably due to aggregation phenomena. MD simulations with two molecules **2** inserted in the aqueous phase show that, after adsorption, they diffuse close to each other and remain side by side at the interface, interacting mostly via their hydrophilic chains (Figures S6 and S7). This mutual orientation of the porphyrins favours dipolar excitonic coupling and should, thus, significantly affect the excited-state properties. Khairutdinov et al. showed that aggregates of free-base phorphyrins in aqueous environments are hardly fluorescent due to efficient internal conversion on the 30 to 200 ps timescale.[58] This study revealed that these aggregates also absorb in both the Soret and Q band regions. The fast dynamic component measured with **2** could, thus, be due to the ground-state recovery of photoexcited aggregates. The faster than expected ns recovery of the SH intensity could be due to the quenching of excited monomers by nearby aggregates, a phenomenon that is well known for xanthene dyes, such as rhodamines, both in bulk solution and at liquid interfaces.[59–62]

Turning now to the dyad, MD simulations with two dyads **1** located in the aqueous subphase point to aggregation as well (Figures S4 and S5). These simulations suggest that the C_{60} sub-units are relatively close, while the porphyrins are located on opposite sides with their planes making an angle of about 80°. Such mutual orientation with near orthogonal porphyrin planes point to negligible dipolar excitonic coupling, contrary to the analogue **2**.

As depicted in Figure 4A, the TR-SSHG profiles measured with **1** also depend on the concentration, but nevertheless differ from those recorded with **2**. Investigations of the excited-state dynamics of **1** in solution revealed that photoexcitation of the porphyrin moiety is followed by the population of an exciplex-like state in 150 fs in both polar and non-polar solvents.[23,24] In the latter, this exciplex decays back to the ground state on a few ns timescale. In the polar benzonitrile, the exciplex transforms in 6.6 ps into a charge-separated state, with the hole and the electron on the H_2TPP and C_{60} sub-units, respectively. This charge-

separated state was found to recombine back to the ground state in 450 ps. The exciplex was mostly detected by its fluorescence that is distinct from that of the porphyrin.[23] However, no strong spectroscopic signature could be found in the transient electronic absorption spectrum. As a consequence, one can assume that photoexcitation of the dyad at the dodecane/water interface also leads to sub-ps population of the exciplex. The slow recovery of the signal at low concentration would be consistent with the ns decay of the exciplex. Its acceleration upon increasing concentration suggests the occurrence of an intermolecular process, that could speed up the repopulation of the ground state and/or lead to the population of another state, X, with $\beta_X > \beta_{S1}$ at the probe wavelength.

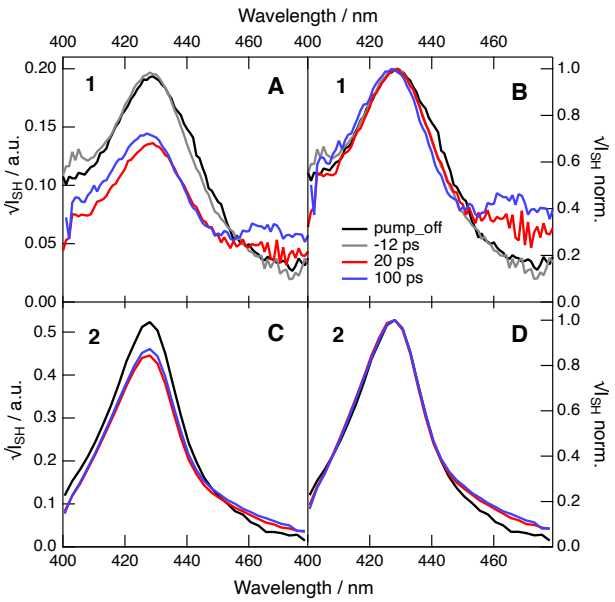

Figure 5: SH spectra (A, C) and intensity-normalised SH spectra (B, D) recorded at different times after 520 nm excitation of the dyad **1** (A, B) and the porphyrin-only reference **2** (C, D) at the dodecane water interface (MMA=4 nm^2).

In order to have a better insight into this, transient SH spectra were recorded between 400 and 480 nm with the pump pulses on. Figure 5A shows that, 20 and 100 ps after excitation, the amplitude of the Soret band is significantly reduced in agreement with the TR-SH profiles, and a new band, more visible at a 100 ps delay, is present above 450 nm. The presence of this band, which is not observed with the reference **2** (Figure 5C), is a strong indication of the population of a state X with a non-zero β at the probe wavelength. Based on the results in bulk solutions,[23,24] the state X is interpreted as the charge-separated state, with the SH band above 450 nm attributed to the radical cation of the porphyrin sub-unit.[63,64] The MD simulations suggest that the dyads are mostly surrounded by dodecane. Therefore they should not experience a local field commensurate with that of a polar solvent. In such case, the exciplex can be expected to decay to the ground state on the ns timescale without undergoing charge separation (CS), in agreement with the TR-SH data at low concentration. We hypothesise that at higher concentrations, intermolecular CS between an excited dyad and a dyad in the ground state takes place, with the hole and the electron located on two different molecules (Figure 6). Based on this, the fast recovery components of $S(t)$ present as higher concentrations should mostly reflect the dynamics of this intermolecular CS. The later process should also be favoured by the aggregation suggested by the MD simulations (Figure S4 and S5) with the relatively close proximity of another C_{60} moieties facilitating electron hopping.

Intramolecular charge recombination (CR) in benzonitrile was reported to take place with a 450 ps time constant.[23,24] The time window of the TR-SSHG experiment does not allow measuring the entire signal recovery. However, intermolecular CR can be expected to be significantly slower than intramolecular CR. Given the relatively high concentration of adsorbed molecules, hopping of the charges to adjacent dyads can in principle compete with geminate recombination.

The interfacial dynamics, summarised in Figure 6, can be compared with that reported for solid films of the dyads prepared with the Langmuir-Blodgett (LB) technique.[22] A CS time constant of 2 ns was estimated from the exciplex lifetime. The authors determined from time-resolved photoelectric measurements that CR occurs on multiple timescales and that the decay of the charge-separated state follows a power law time dependence, $f(t) \propto t^{-\beta}$, with

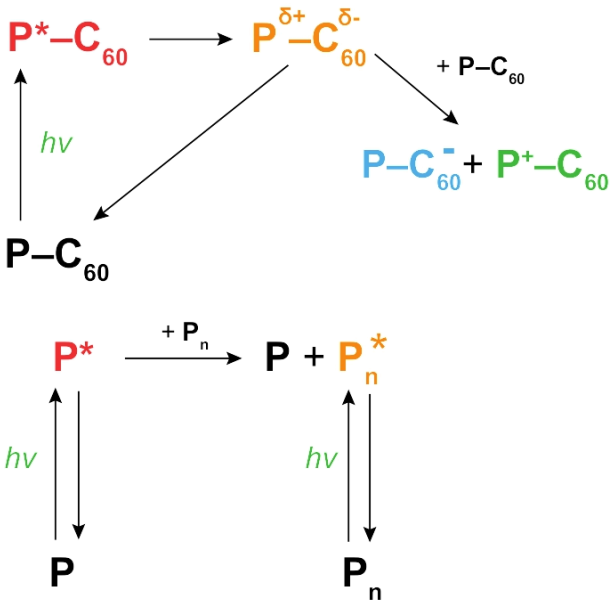

Figure 6: Schemes illustrating the most relevant processes upon photoexcitation of the dyad **1** (top) and the porphyrin reference **2** (bottom) at the dodecane water interface. P stands for the porphyrin and P_n for porphyrin aggregates. For the sake of simplicity, the vertical arrow from P* to P also includes the intersystem crossing to the triplet state and its ensuing decay to the ground state. The ground-state equilibrium for aggregation is also omitted.

β around 0.25. Such behaviour is indicative of lateral diffusion of the charges in the film. Similarly, transient absorption measurements on solid LB films of a dyad similar to **1** but with a phthalocyanine donor revealed intermolecular CS occurring in 35 ps, with CR taking place on the μs timescale.[65]

Therefore, the excited-state dynamics proposed here for the dyad at the dodecane/water interface occurs in a regime that is between that found in bulk solutions, where intermolecular interactions are negligible and solvation drives CS, and that in solid films where there is no formal solvent and intermolecular interactions are dominant.

Conclusions

We have investigated the excited-state properties of an amphiphilic electron donor-acceptor dyad at the dodecane/water interface. Polarisation-resolved SSHG measurements supported by MD simulations revealed significantly different orientations for the dyad and the porphyrin reference at the interface. The orientation is dictated by the presence of the hydrophobic fullerene sub-unit, that causes the dyad to be almost entirely surrounded by dodecane. The location of the dyad at the interface has strong consequence on its excited-state dynamics, because intramolecular charge separation is not operative in such low polarity environment. Instead, photoexcitation of the dyad leads to the population of an excited state with modest charge-transfer character, that decays back to the ground state. However, because the amphiphilic dyad adsorb efficiently, interfacial concentrations enabling self-quenching processes can be easily reached. Based on the SH spectra recorded after photoexcitation, the acceleration of the TR-SH signal recovery observed upon increasing concentration is attributed to an intermolecular charge separation between two dyads.

This investigation illustrates how chemical reactivity at liquid interfaces can differ from that in bulk solution. In addition to favouring intermolecular processes, liquid interfaces also allow for some control of the orientation and position of the adsorbates upon addition of hydrophilic or hydrophobic substituents at specific locations. For example, adding stronger hydrophilic groups on the dyad investigated here could shift its position toward an environment that might be sufficiently polar to enable intramolecular charge separation.

Acknowledgement The authors thanks Dr. Giuseppe Licari for his advices on the MD simulations. The Swiss National Science Foundation (grant 200020-184607) and the University of Geneva are thanked for their financial support.

Supporting Information Available: Analysis of the polarisation-resolved SSHG data, calculation of the hyperpolarisabity MD simulations, time-resolved fluorescence, analysis of the time-resolved SSHG data. All data can be downloaded from

https://doi.org/10.26037/yareta:vo4jtzixorg2jmpw2r2syq3tc4. This material is available free of charge via the Internet at http://pubs.acs.org/.

References

(1) Ball, P. Water as an Active Constituent in Cell Biology. *Chem. Rev.* **2007**, *108*, 74–108.

(2) Volkov, A. G. E. *Liquid Interfaces in Chemical, Biological, and Pharmaceutical Applications*; Marcel Dekker: New York, 2009.

(3) Girault, H. H. In *Electroanalytical Chemistry*; Bard, A. J., Zoski, C. G., Eds.; 2010; Vol. 23; pp 1–104.

(4) Liu, S.; Li, Q.; Shao, Y. Electrochemistry at Micro- and Nanoscopic Liquid/Liquid Interfaces. *Chem. Soc. Rev.* **2011**, *40*, 2236–2253.

(5) Benjamin, I. Reaction Dynamics at Liquid Interfaces. *Annu. Rev. Phys. Chem.* **2015**, *66*, 165–188.

(6) Divya, V.; Sangaranarayanan, M. V. Nanomaterials at Liquid/Liquid Interfaces. A Review. *J. Nanosci. Nanotechnol.* **2015**, *15*, 6863–6882.

(7) Zarbin, A. J. G. Liquid-Liquid Interfaces: a Unique and Advantageous Environment to Prepare and Process Thin Films of Complex Materials. *Mater. Horiz.* **2021**, *8*, 1409–1432.

(8) Narayan, S.; Muldoon, J.; Finn, M. G.; Fokin, V. V.; Kolb, H. C.; Sharpless, K. B. 'On Water': Unique Reactivity of Organic Compounds in Aqueous Suspension. *Angew. Chem., Int. Ed.* **2005**, *44*, 3275–3279.

(9) Klijn, J. E.; Engberts, J. B. F. N. Fast Reactions 'On Water'. *Nature* **2005**, *435*, 746–747.

(10) Jung, Y.; Marcus, R. A. On the Theory of Organic Catalysis 'on Water'. *J. Am. Chem. Soc.* **2007**, *129*, 5492–5502.

(11) Kitanosono, T.; Kobayashi, S. Reactions in Water Involving the 'On-Water' Mechanism. *Chem. Eur. J.* **2020**, *26*, 9408–9429.

(12) Cortes-Clerget, M.; Yu, J.; Kincaid, J. R. A.; Walde, P.; Gallou, F.; Lipshutz, B. H. Water as the Reaction Medium in Organic Chemistry: from our Worst Enemy to our Best Friend. *Chem. Sci.* **2021**, *12*, 4237–4266.

(13) Walker, R. A. Faster Chemistry at Surfaces. *Nat. Chem.* **2021**, *13*, 296–297.

(14) McArthur, E. A.; Eisenthal, K. B. Ultrafast Excited-State Electron Transfer at an Organic Liquid/Aqueous Interface. *J. Am. Chem. Soc.* **2006**, *128*, 1068–1069.

(15) Fedoseeva, M.; Richert, S.; Vauthey, E. Excited-State Dynamics of Organic Dyes at Liquid-Liquid Interfaces. *Langmuir* **2012**, *28*, 11291–11301.

(16) Eisenthal, K. B. Liquid Interfaces Probed by Second-Harmonic and Sum-Frequency Spectroscopy. *Chem. Rev.* **1996**, *96*, 1343–1360.

(17) Brevet, P.-F. *Surface Second Harmonic Generation*; Presses polytechniques et universitaires romandes: Lausanne, 1997.

(18) Simpson, G. J. New Tools for Surface Second-Harmonic Generation. *Appl. Spectrosc.* **2001**, *55*, 16A–32A.

(19) Richert, S.; Fedoseeva, M.; Vauthey, E. Ultrafast Photoinduced Dynamics at Air/Liquid and Liquid/Liquid Interfaces. *J. Phys. Chem. Lett.* **2012**, *3*, 1635–1642.

(20) Tian, C. S.; Shen, Y. R. Recent Progress on Sum-Frequency Spectroscopy. *Surf. Sci. Rep.* **2014**, *69*, 105–131.

(21) Tran, R. J.; Sly, K. L.; Conboy, J. C. Applications of Surface Second Harmonic

Generation in Biological Sensing. *Annu. Rev. Anal. Chem.* **2017**, *10*, 387–414.

(22) Vuorinen, T.; Kaunisto, K.; Tkachenko, N. V.; Efimov, A.; Lemmetyinen, H.; Alekseev, A. S.; Hosomizu, K.; Imahori, H. Photoinduced Electron Transfer in Langmuir-Blodgett Monolayers of Porphyrin-Fullerene Dyads. *Langmuir* **2005**, *21*, 5383–5390.

(23) Chukharev, V.; Tkachenko, N. V.; Efimov, A.; Guldi, D. M.; Hirsch, A.; Scheloske, M.; Lemmetyinen, H. Tuning the Ground-State and Excited-State Interchromophore Interactions in Porphyrin-Fullerene π-Stacks. *J. Phys. Chem. B* **2004**, *108*, 16377–16385.

(24) Chukharev, V.; Tkachenko, N. V.; Efimov, A.; Lemmetyinen, H. Effect of Central Metal on Intra-Molecular Exciplex of Porphyrin-Fullerene Double Linked Dyad. *Chem. Phys. Lett.* **2005**, *411*, 501–505.

(25) Lemmetyinen, H.; Tkachenko, N. V.; Efimov, A.; Niemi, M. Temperature Independent Ultrafast Photoinduced Charge Transfer in Donor-Acceptor Pairs Forming Exciplexes. *J. Phys. Chem. C* **2009**, *113*, 11475–11483, doi: 10.1021/jp901555m.

(26) Kesti, T. J.; Tkachenko, N. V.; Vehmanen, V.; Yamada, H.; Imahori, H.; Fukuzumi, S.; Lemmetyinen, H. Exciplex Intermediates in Photoinduced Electron Transfer of Porphyrin-Fullerene Dyads. *J. Am. Chem. Soc.* **2002**, *124*, 8067–8077.

(27) Efimov, A.; Vainiotalo, P.; Tkachenko, N. V.; Lemmetyinen, H. Efficient Synthesis of Highly Soluble Doubly-Bridged Porphyrin-Fullerene Dyad. *J. Porphyrins Phthalocyanines* **2003**, *07*, 610–616.

(28) Fedoseeva, M.; Fita, P.; Vauthey, E. Excited-State Dynamics of Charged Dyes at Alkane/Water Interfaces in the Presence of Salts and Ionic Surfactants. *Langmuir* **2013**, *29*, 14865–14872.

(29) Richert, S.; Mosquera Vazquez, S.; Grzybowski, M.; Gryko, D. T.; Kyrychenko, A.; Vauthey, E. Excited-State Dynamics of an Environment-Sensitive Push-Pull Diketopyrrolopyrrole: Major Differences between the Bulk Solution Phase and the Dodecane/Water Interface. *J. Phys. Chem. B* **2014**, *118*, 9952–9963.

(30) Licari, G.; Brevet, P.-F.; Vauthey, E. Fluorescent DNA Probes at Liquid/Liquid Interfaces Studied by Surface Second Harmonic Generation. *Phys. Chem. Chem. Phys.* **2016**, *18*, 2981–2992.

(31) Abraham, M. J.; Murtola, T.; Schulz, R.; Pall, S.; Smith, J. C.; Hess, B.; Lindahl, E. GROMACS: High Performance Molecular Simulations through Multi-Level Parallelism from Laptops to Supercomputers. *SoftwareX* **2015**, *1-2*, 19–25.

(32) Hornak, V.; Abel, R.; Okur, A.; Strockbine, B.; Roitberg, A.; Simmerling, C. Comparison of Multiple Amber Force Fields and Development of Improved Protein Backbone Parameters. *Proteins* **2006**, *65*, 712–25.

(33) Lindorff-Larsen, K.; Piana, S.; Palmo, K.; Maragakis, P.; Klepeis, J. L.; Dror, R. O.; Shaw, D. E. Improved Side-Chain Torsion Potentials for the Amber ff99SB Protein Force Field. *Proteins* **2010**, *78*, 1950–8.

(34) Sousa da Silva, A. W.; Vranken, W. F. ACPYPE - AnteChamber PYthon Parser InterfacE. *BMC Res. Notes* **2012**, *5*, 367.

(35) Lee, C.; Yang, W.; Parr, R. G. Development of the Colle-Salvetti Correlation-Energy Formula into a Functional of the Electron Density. *Phys. Rev. B* **1988**, *37*, 785–789.

(36) Frisch, M. J.; Trucks, G. W.; Schlegel, H. B.; Scuseria, G. E.; Robb, M. A.; Cheeseman, J. R.; Scalmani, G.; Barone, V.; Petersson, G. A.; Nakatsuji, H. et al. Gaussian 16 Rev. B.01. **2016**,

(37) Monticelli, L. On Atomistic and Coarse-Grained Models for C60 Fullerene. *J. Chem. Theor. Comput.* **2012**, *8*, 1370–1378.

(38) Chirlian, L. E.; Francl, M. M. Atomic Charges Derived from Electrostatic Potentials: A Detailed study. *J. Comput. Chem.* **1987**, *8*, 894–905.

(39) Jorgensen, W. L.; Chandrasekhar, J.; Madura, J. D.; Impey, R. W.; Klein, M. L. Comparison of Simple Potential Functions for Simulating Liquid Water. *J. Chem. Phys.* **1983**, *79*, 926–935.

(40) Jambeck, J. P.; Lyubartsev, A. P. Derivation and Systematic Validation of a Refined all-Atom Force Field for Phosphatidylcholine Lipids. *J. Phys. Chem. B* **2012**, *116*, 3164–79.

(41) Licari, G.; Cwiklik, L.; Jungwirth, P.; Vauthey, E. Exploring Fluorescent Dyes at Biomimetic Interfaces with Second Harmonic Generation and Molecular Dynamics. *Langmuir* **2017**, *33*, 3373–3383.

(42) Gouterman, M.; Wagniere, G. H.; Snyder, L. C. Spectra of Porphyrins: Part II. Four Orbital Model. *J. Mol.Spectrosc.* **1963**, *11*, 108–127.

(43) Boyd, R. *Nonlinear Optics*, 3rd ed.; Academic Press: Orlando, 2008.

(44) Nagatani, H.; Piron, A.; Brevet, P.-F.; Fermin, D. J.; Girault, H. H. Surface Second Harmonic Generation of Cationic Water-Soluble Porphyrins at the Polarized Water|1,2-Dichloroethane Interface. *Langmuir* **2002**, *18*, 6647–6652.

(45) Nagatani, H.; Samec, Z.; Brevet, P.-F.; Fermin, D. J.; Girault, H. H. Adsorption and Aggregation of meso-Tetrakis(4-carboxyphenyl)porphyrinato Zinc(II) at the Polarized Water|1,2-Dichloroethane Interface. *J. Phys. Chem. B* **2003**, *107*, 786–790.

(46) Fujiwara, K.; Monjushiro, H.; Watarai, H. Total Internal Reflection Second-Harmonic Generation Spectrometer System Optimized for the Liquid/Liquid Interface. *Rev. Sci. Instrum.* **2005**, *76*, 023111, doi: 10.1063/1.1854214.

(47) Kruk, N. N. Nonlinear Optical Properties of Tetrapyrrole Compounds and Prospects for their Application (a Review). *J. Appl. Spectrosc.* **2008**, *75*, 461–482.

(48) Lin, L.; Wang, T.; Lu, Z.; Liu, M.; Guo, Y. In Situ Measurement of the Supramolecular Chirality in the Langmuir Monolayers of Achiral Porphyrins at the Air/Aqueous Interface by Second Harmonic Generation Linear Dichroism. *J. Phys. Chem. C* **2014**, *118*, 6726–6733.

(49) Pavlovich, V. S.; Shpilevsky, E. M. Absorption and Fluorescence Spectra of C60 Fullerene Concentrated Solutions in Hexane and Polystyrene at 77-300 K. *J. Appl. Spectrosc.* **2010**, *77*, 335–342.

(50) Tamburello-Luca, A. A.; Hebert, P.; Brevet, P. F.; Girault, H. H. Resonant-Surface Second-Harmonic Generation Studies of Phenol Derivatives at Air/Water and Hexane/Water Interfaces. *J. Chem. Soc., Faraday Trans.* **1996**, *92*, 3079–3085.

(51) Simpson, G. J.; Westerbuhr, S. G.; Rowlen, K. Molecular Orientation and Angular Distribution Probed by Angle-Resolved Absorbance and Second Harmonic Generation. *Anal. Chem.* **2000**, *72*, 887–898.

(52) Doughty, B.; Rao, Y.; Kazer, S. W.; Kwok, S. J.; Turro, N. J.; Eisenthal, K. B. Probing the Relative Orientation of Molecules Bound to DNA through Controlled Interference using Second-Harmonic Generation. *Proc. Natl. Acad. Sci. USA* **2013**, *110*, 5756–5758.

(53) Svechkarev, D.; Kolodezny, D.; Mosquera-Vazquez, S.; Vauthey, E. Complementary

Surface Second Harmonic Generation and Molecular Dynamics Investigation of the Orientation of Organic Dyes at a Liquid/Liquid Interface. *Langmuir* **2014**, *30*, 13869–13876.

(54) Simpson, G. J.; Rowlen, K. L. An SHG Magic Angle: Dependence of Second Harmonic Generation Orientation Measurements on the Width of the Orientation Distribution. *J. Am. Chem. Soc.* **1999**, *121*, 2635–2636.

(55) Rodriguez, J.; Kirmaier, C.; Holten, D. Optical Properties of Metalloporphyrin Excited States. *J. Am. Chem. Soc.* **1989**, *111*, 6500–6506.

(56) Banerji, N.; Bhosale, S. V.; Petkova, I.; Langford, S. J.; Vauthey, E. Ultrafast Excited-State Dynamics of Strongly Coupled Porphyrin/Core-Substituted-Naphthalenediimide Dyads. *Phys. Chem. Chem. Phys.* **2011**, *13*, 1019–1029.

(57) Taniguchi, M.; Lindsey, J. S.; Bocian, D. F.; Holten, D. Comprehensive Review of Photophysical Parameters (ϵ, Φ_f, τ_s) of Tetraphenylporphyrin (H2TPP) and Zinc Tetraphenylporphyrin (ZnTPP) - Critical Benchmark Molecules in Photochemistry and Photosynthesis. *J. Photochem. Photobiol. C* **2021**, *46*, 100401.

(58) Khairutdinov, R. F.; Serpone, N. Photoluminescence and Transient Spectroscopy of Free Base Porphyrin Aggregates. *J. Phys. Chem. B* **1999**, *103*, 761–769.

(59) Penzkofer, A.; Lu, Y. Fluorescence Quenching of Rhodamine 6G in Methanol at High Concentration. *Chem. Phys.* **1986**, *103*, 399–405.

(60) Isak, S. J.; Eyring, E. M. Fluorescence Quantum Yield of Cresyl Violet in Methanol and Water as a Function of Concentration. *J. Phys. Chem.* **1992**, *96*, 1738–1742, doi: 10.1021/j100183a045.

(61) Fita, P.; Fedoseeva, M.; Vauthey, E. Hydrogen-Bond-Assisted Excited-State Deactivation at Liquid/Water Interfaces. *Langmuir* **2011**, *27*, 4645–4652.

(62) Fedoseeva, M.; Letrun, R.; Vauthey, E. Excited-State Dynamics of Rhodamine 6G in Aqueous Solution and at the Dodecane/Water Interface. *J. Phys. Chem. B* **2014**, *118*, 5184–5193.

(63) Paliteiro, C.; Sobral, A. Electrochemical and Spectroelectrochemical Characterization of Meso-Tetra-Alkyl Porphyrins. *Electrochim. Acta* **2005**, *50*, 2445–2451.

(64) Aleman, E. A.; Manriquez Rocha, J.; Wongwitwichote, W.; Godinez Mora-Tovar, L. A.; Modarelli, D. A. Spectroscopy of Free-Base N-Confused Tetraphenylporphyrin Radical Anion and Radical Cation. *J. Phys. Chem. A* **2011**, *115*, 6456–6471.

(65) Lehtivuori, H.; Kumpulainen, T.; Efimov, A.; Lemmetyinen, H.; Kira, A.; Imahori, H.; Tkachenko, N. V. Photoinduced Electron Transfer in Langmuir-Blodgett Monolayers of Double-Linked Phthalocyanine-Fullerene Dyads. *J. Phys. Chem. C* **2008**, *112*, 9896–9902.

TOC Graphic